No-Reference JPEG Image Quality Assessment Using Haar Wavelet Decomposition

Irwan Prasetya Gunawan[1] and **Antony Halim**[2], Non-members

ABSTRACT

This paper presents a novel method of no-reference image quality assessment for JPEG encoded images by means of multiresolution analysis using Haar wavelet decomposition. The proposed method takes advantage of the fact that JPEG encoded images are usually contaminated with blockiness artifacts. Blockiness artifact is modeled as a particular edge structure that transforms into a different edge structure when edge detection algorithm is applied. Subsequently after edge detection is performed, a 3-level Haar Wavelet Transform (HWT) is employed to construct an edge map, from which some features are derived. These features give meaningful information for blockiness distortions identification and quality assessment. The proposed quality metric was tested against publicly available JPEG subset of LIVE Image Database, whilst the detection algorithm was evaluated subjectively in terms of how well the automatic detection agrees with human's perceived view. The detection algorithms as well as the proposed JPEG quality metric demonstrate satisfying performances.

Keywords: No-Reference, Image, Quality Assessment, Haar, wWvelet, Blockiness

1. INTRODUCTION

Compression is indispensable in various digital image and video applications nowadays. Its purpose is to reduce bit rate requirement of the signals. Ideally, this should be done without compromising the visual quality of the compressed image/video. However, in reality, compression or encoding process may introduce unique visual impairments to the picture and consequently degrades the quality. In some applications, a perceived quality of digital image or video is very important. A typical multimedia system may enhance and restore digital images prior to use them in subsequent applications. By measuring the per-ceived quality of digital image, the system can dynamically adjust the enhancement and restoration parameters to generate better quality image. Subjective quality assessment is traditionally used to measure the perceived quality. Unfortunately, subjective evaluation is impractical for real-time applications because it is time consuming, laborious, and expensive. For that reason, objective quality assessment methodologies are usually preferred than the subjective ones.

The objective quality assessment can be categorized into three different approaches: 1) Full Reference (FR) model such as traditional peak-signal-to-noise ratio (PSNR), Universal Quality Index (UQI) [1], Structural Similarity (SSIM) [2], human visual system (HVS) based wavelet domain analysis [3], neural network approach [4], and modifications of other FR models in wavelet sub-bands [5], all of which require the availability of the original image as a reference to perform quality evaluation; 2) Reduced Reference (RR) model, such as Local Harmonic Strength (LHS) proposed in [6], which uses some features extracted from the original image to perform quality assessment; and 3) No-Reference (NR) model, which uses no additional information whatsoever when performing the evaluation. Some examples of NR methods can be found in [7–11].

The NR approach is attractive compared to the other two because it does not require any information with respect to the original, undistorted picture during evaluation process. It is very practical and suitable for typical applications that do not have the luxury of access to the reference image information. However, to some degree, the practicality of NR model depends on prior knowledge of the distortion that could be present on the image.

For example, in JPEG coded images (and in most block-based video compression systems such as H.263 or MPEG-2) blockiness distortion is the dominant artifact that impairs picture quality. It is characterized by the visibility of the underlying block structure as a result of coarse quantization of spatial frequency components during the encoding process [12]. Blockiness appears as visible discontinuities at the boundary of adjacent blocks of 8×8 pixels, as well as sudden intensity changes in uniform region. Such artificial block boundaries might appear in the images at low bit rates. Due to these characteristics, it is

usually easier to perform blockiness distortion measure by utilizing frequency analysis, Discrete Cosine Transform (DCT), or spatial analysis. Examples of such analyses are NPBM in [7, 9] and blockiness identification in compressed data [13] using the Laplacian model of DCT, to name a few.

Encoding method other than JPEG, such as wavelet-based JPEG 2000, is also available. JPEG 2000 differs from JPEG in terms of the distortions introduced in the compressed image; e.g., blur and ringing impairments. Wavelet-based analysis is considered more suitable for quality assessment of JPEG 2000 encoded images. For example, quality assessment methods presented in [3–5] use wavelet-based multi-resolution approach in a full-reference manner. In [3], local contrast is re-defined by means of wavelet coefficients at different resolutions, and the re-defined contrast is subsequently used to develop a fidelity measure based on perceptual differences. A neural network approach to wavelet-based image quality assessment is presented in [4]; this is a direct application of neural network to the existing works of [1, 2] using a full-reference framework. In [5], the application of PSNR and Picture Quality Score (PQS) metrics in wavelet sub-bands are investigated. In another work [10], an NR model is proposed to assess specific wavelet-based coded image; it uses mean squared error (MSE) reduction estimation for an embedded wavelet image coder such as set portioning in hierarchical tree (SPIHT) coding algorithm. Such wavelet-based analyses have emerged as powerful tools to analyse information on the image because of its ability to perform the analysis at various scales. This is similar to conventional frequency analysis; however, unlike the frequency analysis, wavelet-based analysis preserves the spatial information of the signal.

Since JPEG encoding and other similar DCT block-based compression methods are still widely used nowadays, we focus our attention to this particular type of encoded images in this paper. Different from previous works described above, in this paper we proposed a wavelet-based NR quality assessment method for JPEG images by employing a 3-level Haar Wavelet Transform (HWT) to decompose edges information of an image and derive certain features based on the resulting wavelet detail coefficients. We adopted a method originally proposed by [14] which used the HWT to classify blurred images against unblurred ones. Since our purpose is to measure and identify blockiness distortions in JPEG images, we decided to choose decomposition based on Haar wavelet due to its simple and fast discrete implementation. We considered Haar wavelet was appropriate for our analysis since our proposed method does not require specific characteristic of wavelet function such as arbitrary regularity of Daubechies wavelet [15] or linear phase for exact reconstruction in Biorthogonal wavelet [15], for example. We also reckoned 3-level

decomposition was sufficient to extract useful features for our JPEG image quality assessment and blockiness distortions identification method. In retrospect, our method is similar to [3] in terms of using constrast information, however ours was used in the absence of any reference information. We will show in the subsequent section the rationale of such arrangement.

This paper is organized as follows. We describe our proposed method in more detail in Section 2. Subsequently, experimental results using LIVE JPEG Image Database [16] is presented in Section 3. Finally, we give conclusions to our works in Section 4.

2. METHOD

Our proposed method is divided into four parts as follows:

1. Pre-processing stage. This part starts with edge detection, followed by spatial masking and texture filtering process to the detected edge image. Median filtering may also subsequently be used to remove unwanted noise. Edges are classified according to [14]; however, for our blockiness distortion quality measurement we only used two of them, namely Astep and Roof edge structures. We modeled the blockiness distortion as an Astep edge structure (Figure 1(a)) having a low-to-moderate intensity variation. We observed that when we applied Sobel operators [17] to detect edges on the image, this particular type of edge structure will transform into Roof edge structure (Figure 1(b)), also having low-to-moderate transition. Based on our experiment and observation which will be described later, we devised some new rules to characterize the Roof edge structure that corresponds to blockiness distortion on the image.

2. Feature extraction stage. This part derives some features from the edge image using 3-level HWT. An edge map is constructed using horizontal and vertical wavelet detail coefficients. From this edge map, useful features are constructed by finding some local maxima in pre-defined window sizes; e.g., 8×8, 4×4, and 2×2 pixels for level-1, -2, and -3 decompositions, respectively.

3. Blockiness distortions identification. This part is mainly responsible for locating and identifying blockiness artifacts on the images using the information from the features that have been extracted in the
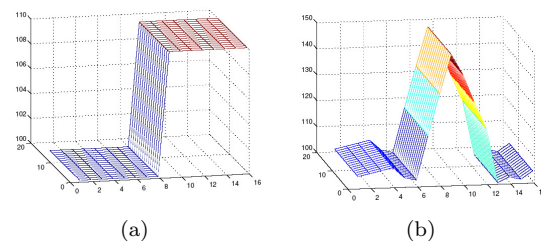

Fig.1: (a) Basic Astep edge structure and (b) Basic Roof edge structure from [14]
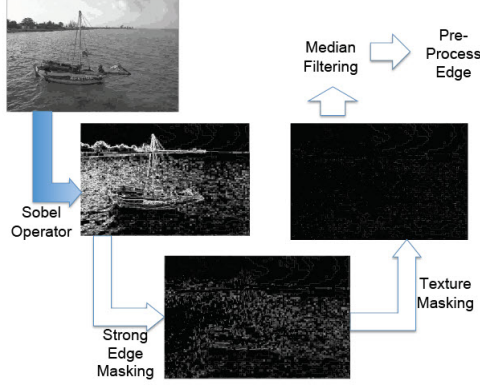
Fig.2: *Illustration of Pre-Process Stage. The first input is a grayscale image transformed from original Sailing1 category image from LIVE JPEG Database. A Sobel Operator applied to the input and generate the edge image. The edge image then is masked (spatial masking process). After the spatial masking process, the image undergo a texture filtering process. Additionally, a median filter is applied to the image and the final pre-processed image is generated.*

previous stage. The blockiness artifact can be characterized by wavelet coefficients computed from the HWT of edge image.

4. Quality metric calculation. This final part is responsible for computing the quality score of the JPEG image based on the extracted features.

The detailed explanation of the method is given in the following sub sections.

2.1 Pre-Processing Stage

An illustration of pre-processing stage is given in Figure 2. Consider an image $I(m,n)$ of size $M \times N$, where M and N represent its width and height, respectively, and $m \leq M, n \leq N$. We compute the edge of the image, $E(m,n)$, by applying the horizontal and vertical Sobel operators [17] G_x and G_y, respectively:

$$G_x = \begin{pmatrix} -1 & 0 & 1 \\ -2 & 0 & 2 \\ -1 & 0 & 1 \end{pmatrix} \tag{1}$$

$$G_y = \begin{pmatrix} 1 & 2 & 1 \\ 0 & 0 & 0 \\ -1 & -2 & -1 \end{pmatrix}. \tag{2}$$

The edge image $E(m,n)$ is calculated by applying each of the G_x and G_y to the image $I(m,n)$ and combining both the horizontal edge $H(m,n)$ and vertical edge $V(m,n)$ according to the following equations:

$$H(m,n) = I(m,n) * G_x \tag{3}$$

$$V(m,n) = I(m,n) * G_y \tag{4}$$

$$E(m,n) = \sqrt{H(m,n)^2 + V(m,n)^2}. \tag{5}$$

The $E(m,n)$ is then converted into image data for subsequent process. After the edge image is generated, we need to perform spatial masking by removing any strong edges having intensities above a certain threshold δ_{strong}. We use δ_{strong} to differentiate visible strong edges from the weak ones. In our method, we assume that the former have much higher intensity than the latter.

The spatial masking is applied for three pixels in both directions of vertical neighbourhood with respect to the reference edge pixel. This part is mainly responsible to introduce simplified Human Visual System (HVS) characteristics [18] to the algorithm. It is important because strongly visible edges may hide blockiness artifacts from human vision. This is a particular property of the HVS that will surely affect the identification and the quality metric derived later on. Therefore, any strongly visible edges on the image must be compensated first before getting any further treatment. The spatial masking is illustrated by the equation below:

$$E(m, n+k)$$
$$= \begin{cases} 0, & E(m,n) > \delta_{strong} \\ E(m,n+k), & E(m,n) \leq \delta_{strong} \end{cases} \tag{6}$$

for $-3 \leq k \leq 3$. We decided to extend the masking for three pixels in both directions of the vertical neighbourhood to compensate the spread characteristics of the strongly visible edges. We considered three pixels are sufficient to simulate the masking effect of dominant edges to their neighbourhood [12]. We only selected the vertical neighbourhood of the reference edge pixel to be masked because the horizontal orientation was automatically masked when we repeated the vertical masking of adjacent pixels.

The next part of the proposed method is texture masking. It is used to reduce misclassification error that may occur in the identification process due to random characteristics of texture. This part is also another contribution of HVS to the proposed method, since textural structures may hide the visibility of blockiness artifacts from human vision. In this texture masking, we define an entropy threshold $\delta_{entropy}$ to measure the busyness of the observed block. The entropy ε is calculated for every 8×8 blocks of the edge images $B_{i,j}$, $i \leq M/8, j \leq N/8, B_{i,j} \in E$. Additional 8×8 grid mask g is applied for every $B_{i,j}$ to shift the focus of entropy calculation to the area inside the grid boundary and excludes blockiness distortion boundary from the computation of block busyness.

The grid mask g can be expressed as:

$$g = \begin{pmatrix} 0 & 0 & 0 & 0 & 0 & 0 & 0 & 0 \\ 0 & 1 & 1 & 1 & 1 & 1 & 1 & 0 \\ 0 & 1 & 1 & 1 & 1 & 1 & 1 & 0 \\ 0 & 1 & 1 & 1 & 1 & 1 & 1 & 0 \\ 0 & 1 & 1 & 1 & 1 & 1 & 1 & 0 \\ 0 & 1 & 1 & 1 & 1 & 1 & 1 & 0 \\ 0 & 1 & 1 & 1 & 1 & 1 & 1 & 0 \\ 0 & 0 & 0 & 0 & 0 & 0 & 0 & 0 \end{pmatrix}. \qquad (7)$$

The entropy ε itself is calculated from the histogram of the block by applying the following equation:

$$\varepsilon(B, g) = - \sum \left[p(B \cdot g) \times \log_2 p(B \cdot g) \right] \qquad (8)$$

where p represents the histogram function. Higher entropy of a block corresponds to higher activity within the block, and it is more than likely that it is a textured area. We cannot set the $\delta_{entropy}$ as zero since it will overfilter the texture masking process. Hence, it is better to set the $\delta_{entropy}$ as small as possible and close to zero since any blockiness distortion that appears will remove the detail of a block and thus reducing the entropy of the block. The texture masking algorithm compares the entropy ε with the $\delta_{entropy}$ according to the following equation:

$$B_{i,j} = \begin{cases} 0_{ij}, & \varepsilon > \delta_{entropy} \\ B_{ij}, & \varepsilon \leq \delta_{entropy}. \end{cases} \qquad (9)$$

The pre-processed edge image, $\widehat{E}_p(m, n)$ is then constructed by concatenating the blocks from texture masking process:

$$\widehat{E}_p(m, n) = \begin{pmatrix} B_{1,1} & B_{1,2} & \cdots & B_{1,j} \\ B_{2,1} & B_{2,2} & \cdots & B_{2,j} \\ \vdots & \vdots & \ddots & \vdots \\ B_{(i-1),1} & B_{(i-1),2} & \cdots & B_{(i-1),j} \\ B_{i,1} & B_{i,2} & \cdots & B_{i,j} \end{pmatrix}. \qquad (10)$$

Additionally, median filtering can also be used to remove unwanted noise in $\widehat{E}_p(m, n)$ that may still be left on the pre-processed edge image after texture filtering.

2.2 Feature Extraction

When the pre-processed edge image $\widehat{E}_p(m, n)$ is ready, we need to extract some features from it for further processing. We extract local maxima from an edge map of the pre-processed image. The edge map is constructed from the detail coefficients of the HWT decomposition of the pre-processed image. The local maxima feature, based on [14], is used for quality assessment and blockiness distortion identification purposes. The followings describe our proposed feature extraction method in detail.

First, we compute the 3-level Haar Wavelet Decomposition (HWD):

$$[A_i | H_i | V_i | D_i](k_i, l_i) = HWD(\widehat{E}_p(m, n)) \qquad (11)$$

where $i = 1, 2, 3$ represent the decomposition level. $H_i(k_i, l_i)$, $V_i(k_i, l_i)$, and $D_i(k_i, l_i)$ are horizontal detail coefficients (LH subband), vertical detail coefficients (HL subband), and diagonal detail coefficients (HH subband) at decomposition level i, respectively. We use A_{i-1} as the input for HWD at level i, given $A_0 = \widehat{E}_p(m, n)$

We construct the edge map ρ_{map_i} for each level of decomposition i from the horizontal and vertical detail coefficients, $H_i(k, l)$ and $V_i(k, l)$. We exclude the diagonal detail coefficients since in JPEG encoded images the blockiness pre-dominantly appears in horizontal and vertical direction. The edge map ρ_{map_i} is constructed by applying the following equation:

$$\rho_{map_i}(k_i, l_i) = \sqrt{|H_i(k_i, l_i)|^2 + |V_i(k_i, l_i)|^2} \qquad (12)$$

for $i = 1, 2, 3$. After we get the edge map ρ_{map_i} for each decomposition level, we calculate the local maxima feature $\tilde{\phi}_{pq_i}$ of the edge map as follows: for a $K_i \times L_i$ edge map at decomposition level i, the feature matrix $\tilde{\phi}_{pq_i}$ is computed by finding the local maxima for every $2^{(4-i)} \times 2^{(4-i)}$ non-overlapped window $\tilde{W}_{pq}$ at each level of decomposition i, given $p \leq \lfloor K_i/2^{(4-i)} \rfloor, q \leq \lfloor L_i/2^{(4-i)} \rfloor$ and p, q represent block coordinates tha correspond to the non-overlapped window $\tilde{W}_{pq}$. This can be summarized as follows:

$$\tilde{\phi}_{pq_i} = \arg \max(\tilde{W}_{pq}); \quad i = 1, 2, 3. \qquad (13)$$

Subsequently, the local maxima feature matrix $\widehat{\phi}_i^{max}$ is constructed by collecting each of the $\tilde{\phi}_{pq_i}$ according to

$$\widehat{\phi}_i^{max}(p, q) = \begin{pmatrix} \tilde{\phi}_{11_i} & \tilde{\phi}_{12_i} & \cdots & \tilde{\phi}_{1q_i} \\ \tilde{\phi}_{21_i} & \tilde{\phi}_{22_i} & \cdots & \tilde{\phi}_{2q_i} \\ \vdots & \vdots & \ddots & \vdots \\ \tilde{\phi}_{(p-1)1_i} & \tilde{\phi}_{(p-1)2_i} & \cdots & \tilde{\phi}_{(p-1)q_i} \\ \tilde{\phi}_{p1_i} & \tilde{\phi}_{p2_i} & \cdots & \tilde{\phi}_{pq_i} \end{pmatrix}. \qquad (14)$$

This feature matrix $\widehat{\phi}_i^{max}$ will be used to identify any possible locations of blockiness artifact and to assess the quality of the images.

2.3 Blockiness Distortions Identification

On the edge image $\widehat{E}_p(m, n)$, the blockiness artifacts can be modeled as a Roof edge structure [14] due to gradient transformation, and characterized by $\widehat{\phi}_i^{max}$ features. Referring to [14], the criteria to characterize Roof edge structure in the image is $\widehat{\phi}_1^{max}(p, q) < \widehat{\phi}_2^{max}(p, q) < \widehat{\phi}_3^{max}(p, q)$. If this criteria holds, then a Roof edge structure is identified at coordinate p, q.

This rule, however, is good if it was applied to an ideal blockiness. We found that the rule set out by [14] did not really work well when randomness occur in the block. Therefore, we propose a modified version of the rule to characterize Roof edge structure at coordinate p, q based on our experiments and observation summarized in Table 1.

Since we know that $\tilde{\phi}_{pq_i}$ is computed for every $2^{(4-i)} \times 2^{(4-i)}$ non-overlapped window $\tilde{W}_{pq}$, hence, the local maxima will be computed for every 8×8, 4×4, and 2×2 non-overlapped window at level-1, level-2, and level-3 decompositions, respectively. Based on the characteristics of wavelet decomposition [19] that downsamples the original signal by a factor of 2, each $\tilde{\phi}_{pq_i}$ will refer to a certain non-overlapped block of 16×16 pixels in the input image at block coordinate p, q. We then conducted an experiment that simulated the computation of $\tilde{\phi}_{pq_i}$ for various 16×16 Roof edge structure blocks. The simulation decomposed various 16×16 Roof edge structure blocks and computed the $\tilde{\phi}_{pq_i}$ for each block at different level of decomposition i. Note that for 16×16 block, $p = 1, q = 1$; therefore we generalized the $\tilde{\phi}_{pq_i}$ as $\tilde{\phi}_i$ for this experiment. We collected the data of $\tilde{\phi}_i$ by varying the intensity range of the Roof edge structure. We also introduced some randomness to the Roof edge structure to simulate how the computation of $\tilde{\phi}_i$ was affected. Table 1 shows some of our experimental results.

Referring to Table 1, we can see that in an ideal Roof edge structure with no randomness, the value of $\tilde{\phi}_2$ and $\tilde{\phi}_3$ will always be same. However, when a certain randomness structure appears in the block, the value of $\tilde{\phi}_2$ and $\tilde{\phi}_3$ will be different although there is no strict pattern as to whether $\tilde{\phi}_2 > \tilde{\phi}_3$ or the other way around. From the simulation we observed that the value $\tilde{\phi}_2$ and $\tilde{\phi}_3$ will always have small differences. In addition, the value of $\tilde{\phi}_1$ will vary through the range of maximum and minimum intensities occurred in the block.

Based on the simulation results summarized in Table 1, we devised a rule to define blockiness distortions characteristic on the image. As we dealt with images having randomness in terms of intensities, our proposed rule was designed to compensate that characteristic yet still preserving the ability to identify the blockiness artifacts on the image. We also took into consideration that $\tilde{\phi}_1$ can also be affected by the different intensity range characteristics of the image. In general, we found that blockiness artifacts occurred if small differences exist between $\tilde{\phi}_i$ at different decomposition level i. Based on Table 1 we also found that the required maximum decomposition level to characterize blockiness artifact was three. Only three decomposition levels were needed since we could see that blockiness can be characterized effectively using $\tilde{\phi}_2$ and $\tilde{\phi}_3$. Fewer decomposition level will make the blockiness identification process difficult to be exe-

Table 1: $\tilde{\phi}_i$ characteristics of various Roof edge structures with varying intensities and certain randomness. R correspond to max randomness changes can occurred in the block. Min. I is the minimum intensities of the Roof edge while Max. I is the maximum intensities (peak) of the Roof edge.

R	Min. I	Max. I	$\tilde{\phi}_1$	$\tilde{\phi}_2$	$\tilde{\phi}_3$
0	20	30	5	15	15
0	20	40	10	30	30
0	20	70	25	75	75
0	20	80	30	90	90
0	20	90	35	105	105
0	100	110	5	15	15
0	100	120	10	30	30
0	100	130	15	45	45
0	100	140	20	60	60
0	100	150	25	75	75
0	100	160	30	90	90
0	100	170	35	105	105
0	100	100	0	0	0
5	20	30	10.2	22	19.22
5	20	40	17.51	37.77	32.42
5	20	70	30	79.06	79.16
5	20	80	36.53	94.25	92.8
5	20	90	41.01	109.77	113.52
5	110	120	9.62	18.03	14.51
5	110	130	17	33.38	30.68
5	110	140	21.02	48.3	47.91
5	110	150	25.02	64.02	62.64
5	110	160	31.06	78	76.02
5	110	170	33.02	93.55	91.33
10	30	40	16.28	21.75	20.74
10	30	50	23.35	41.3	40.18
10	30	60	32.5	62.55	56.74
10	30	70	36.01	66.15	63.88
10	30	80	35.78	84.14	83.18
10	100	110	17.56	25.94	19.85
10	100	120	21.69	39.7	28.04
10	100	130	26.62	58.67	54.63
10	100	140	27.07	74.88	65.5
10	100	150	37.58	78.63	82.8
10	100	160	40.31	102.87	95.48
10	100	170	48.01	110.49	106.32

cuted. Higher decomposition level (more than three levels) is not effective and does not provide additional benefit either.

Our proposed criteria to identify Roof edge (and consequently leading to identifying blockiness artifacts) is that blockiness artifact occur when there are absolute minimum differences between $\widehat{\phi}_i^{max}(p, q)$ at different level i whose values are below a certain threshold δ_{diff}. The value of δ_{diff} is very important since it compensates the influence of the random intensities characteristics of the block in the image to the $\widehat{\phi}_i^{max}(p, q)$ at various different level i. It

also serves as a compensation of how difficult blockiness artifacts will be detected, for example, when the blockiness artifacs are not clearly visible or located around edges or textured areas. In other words, it can be used to control the perceptual visibilities of the blockiness artifacts.

For algorithmic approach, we compute the difference between $\widehat{\phi}_i^{max}(p,q)$ at various different levels, either level 1 and 2, level 2 and 3, or level 1 and 3, and compute the minima amongst them, such as followed:

$$\widehat{\theta}_{21}^{max}(p,q) = |\widehat{\phi}_2^{max}(p,q) - \widehat{\phi}_1^{max}(p,q)| \qquad (15)$$

$$\widehat{\theta}_{32}^{max}(p,q) = |\widehat{\phi}_3^{max}(p,q) - \widehat{\phi}_2^{max}(p,q)| \qquad (16)$$

$$\widehat{\theta}_{31}^{max}(p,q) = |\widehat{\phi}_3^{max}(p,q) - \widehat{\phi}_1^{max}(p,q)| \qquad (17)$$

$$\widehat{\theta}^{max}(p,q) = \arg \ \min(\{\widehat{\theta}_{21}^{max}, \widehat{\theta}_{32}^{max}, \widehat{\theta}_{31}^{max}\}(p,q)). \qquad (18)$$

Following our argument in the previous paragraph, blockiness artifacts are identified if the minimum difference $\widehat{\theta}^{max}$ is below the difference threshold δ_{diff}. Since Haar Wavelet Decomposition maintains spatial information on the image, we are able to construct a binary mask M_b to pinpoint the location of the blockiness artifacts. A value of M_b will correspond to a 16×16 block, similar to $\widehat{\phi}_i^{max}(p,q)$, due to downsampling characteristics of the wavelet decomposition as described above. M_b is constructed simply by comparing the $\widehat{\theta}^{max}$ with δ_{diff} as illustrated in the following equation:

$$M_b(p,q) = \begin{cases} 0, & \widehat{\theta}^{max}(p,q) > \delta_{diff} \\ 1, & \widehat{\theta}^{max}(p,q) \le \delta_{diff}. \end{cases} \qquad (19)$$

After we identify all possible locations of blockiness artifacts, we also need to anticipate any flat areas on the images due to characteristics similarity of flat area with blockiness artifacts in terms of minimum difference amongst different level of $\widehat{\phi}^{max}$. We found that flat areas can be differentiated by examining the value of $\widehat{\phi}^{max}$ which will be very small and goes below a certain threshold δ_{flat} in every decomposition level. By applying this principle, we can construct another binary mask for flat area, M_f, such as the following equation:

$$M_f(p,q) = \begin{cases} 1, & \{\widehat{\phi}_1^{max}, \widehat{\phi}_2^{max}, \widehat{\phi}_3^{max}\}(p,q) > \delta_{flat} \\ 0, & \{\widehat{\phi}_1^{max}, \widehat{\phi}_2^{max}, \widehat{\phi}_3^{max}\}(p,q) \le \delta_{flat}. \end{cases} \qquad (20)$$

In our case, we set $M_f(p,q) = 0$ if the corresponding area is identified as flat area.

The final mask for blockiness detection is then constructed by applying element-wise logical operator AND between M_b and M_f as follows:

$$\widehat{M} = M_b \ \& \ M_f. \qquad (21)$$

Finally, we can identify and pinpoint the location of blockiness artifacts by mapping the final mask $\widehat{M}$ to the image $I(m,n)$. Note that each element of $\widehat{M}$ corresponds to a certain 16×16 pixels block in $I(m,n)$.

2.4 Quality Metric Calculation

To calculate the quality metric of an image, we need to measure the degree of blockiness on the image based on $\widehat{\phi}^{max}$ feature. Our proposed quality assessment method uses all possible locations of the distortions that have been identified and measures the degree of these distortions to compute the objective quality metric. Referring to Table 1, we used the $\widehat{\phi}_1^{max}(p,q)$ as a structural information to measure the degree of the distortions that occur on the image based on the fact that $\widehat{\phi}_1^{max}(p,q)$ corresponds to the range of pixel intensities in the block, and hence to the strength of the distortion itself. We also took into account that some distortions can be very sensitive and not visible to human viewers because these distortions only have minor changes in intensities.

Hence, we define a distortion weight matrix $\omega(p,q)$ as follows:

$$\omega(p,q) = \begin{cases} 0.01, & M_b(p,q) = 0 \\ 1, & M_b(p,q) = 1. \end{cases} \qquad (22)$$

The distortions weight $\omega(p,q)$ corresponds to all possible distortions that are identified on the image. In this case, we considered flat area as a possible distortion that can degrade the quality of the image. We took flat area into consideration due to the fact that in most severely compressed JPEG images, blockiness artifacts are usually followed by flat uniform area. This is consistent with the findings in [3] which shows that blockiness distortion is also more dominant in flat or smooth region with slow slope. A small, default value of 0.01 is given to $\omega(p,q)$ if no possible distortions are identified, whilst unity will be given if a possibility of distortions occur, which, in this case could be either blockiness or flat distortions. Note that we give 0.01 as a simple offset to prevent the quality metric pooling to take a logarithmic of zero value. Such condition can occur when an image has no possible distortions.

The quality metric will be derived with the help of structural information of the image based on $\widehat{\phi}_1^{max}(p,q)$. First, a raw quality metric q_m is computed by taking the sum of the element-wise matrix multiplication between structural information that represents the degree of blockiness $\widehat{\phi}_1^{max}(p,q)$ with the distortions weight matrix $\omega(p,q)$ as follows:

$$q_m = \log_{10}\left(\left[\sum_p \sum_q \left\{\omega(p,q).\widehat{\phi}_1^{max}(p,q)\right\}\right]\right). \qquad (23)$$

Then, the raw quality metric q_m is calibrated using non-linear regression to map its value to the subjective data [20]. The proposed quality assessment method uses a 4-parameters logistic curve equation for the fitting. The final quality metric $\tilde{q}_m$ is then
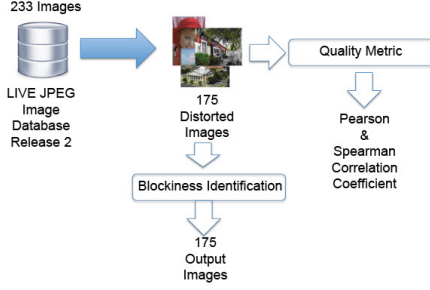
Fig.3: *Experimental Setup. From 233 JPEG Images in LIVE JPEG Database, 175 distorted images were chosen. For blockiness identification experiments the algorithm will produce 175 output images with blockiness artifacts identification results. For the quality metric experiments, the Pearson and Spearman correlation between DMOS and the objective quality metric were computed.*

given by the following equation:

$$\tilde{q}_m = \frac{b_1 - b_2}{1 + exp\left\{\frac{b_3 - q_m}{|b_4|}\right\}} + b_2 \qquad (24)$$

where b_1, b_2, b_3, and b_4 are the parameters of the logistic curve to be estimated using the subjective data. The Pearson and Spearman correlation coefficients will be used to assess the final objective quality metric $\tilde{q}_m$.

3. EXPERIMENTAL RESULTS

We tested the proposed method using LIVE JPEG Image Database Release 2 [16]. The LIVE JPEG Image Database consists of 29 categories of highly textured images annotated with Difference Mean Opinion Score (DMOS) subjective data for each image. DMOS is the arithmetic mean of the difference between the score given to the degraded image and the score given to the reference one. The database uses *imwrite* function from MATLAB to generate the JPEG images [16]. The total number of JPEG images in the database is 233 images, where 175 of them are compressed images ranging from good quality (almost the same as the original) to bad quality. We then used the 175 compressed images in the database to conduct our experiments. Figure 3 gives an illustration on the experimental setup in this research. All the parameters explained in the previous section were adjusted empirically based on the experiment and observation.

The δ_{strong} parameter was set to classify strong edge to perform spatial masking. We set the δ_{strong} to 170 based on our observation that usually strong edges occupied high intensities whereas blockiness distortions strength occupied the image with pixel intensities lower than 170.

The $\delta_{entropy}$ was set based on experimental observation to the texture filtering process. Since the

texture filtering was applied in 8×8 block, thus the $\delta_{entropy}$ had a very limited small value. If we set the $\delta_{entropy}$ to 0, it would cause over-filtering as described in the previous section. Hence, we set $\delta_{entropy}$ to 0.25 as a threshold to distinguish textural structures from the blockiness distortions. The $\delta_{entropy}$ value serves as a maximum entropy that a particular block can tolerate. It can detect textural activities based on the fact that textural structures lead to higher entropy.

The δ_{flat} parameter was used to distinguish flat area from blockiness distortions. We set δ_{flat} based on experimental observation as summarized in Table 1. We assumed a particular block as flat area when the block exhibited small variation in intensities. Referring to Table 1 we can see that when the intensities range is low (around 10), each features $\widehat{\phi}_i^{max}(p, q)$ at different level i will have small value. Therefore we define $\delta_{flat} = 25$ as the maximum value that $\widehat{\phi}_i^{max}(p, q)$ can have at each level to classify the block as flat area.

Finally, we also set the value of δ_{diff} to compensate the characteristic of pixel intensities in the block that may affect $\widehat{\phi}_i^{max}(p, q)$. We set $\delta_{diff} = 30$ by referring to Table 1 when a block has a randomness of 10 and the differences are varied and increased. The $\delta_{diff} = 30$ is a limit to the maximum differences between the features for the block to be classified as blockiness distortions.

From our experiment, the parameters mentioned above were the combinations that yielded the best result.

3.1 Blockiness Identification

We evaluated our proposed blockiness identification method by conducting our own subjective experiment. In the test, viewers were subjected to a pair of images displayed side-by-side on monitor. One of the image is the test image (for example, Fig 4(a)) which may or may not contain blockiness distortion whilst the other one is the same image superimposed with the identification results of the proposed algorithm (Fig. 4(b)). For each pair of these images, the viewers must record a performance score based on how close the results of the identification algorithm correspond with the viewers' opinion. Viewers' opinion regarding the appearance of blockiness distortion on the test image may vary from one person to another. Good performance score will be recorded if the results of the identification algorithm agree with viewers' opinion.

Figure 5 illustrates the scoring convention of the subjective experiment. Perfect score (100) is given if the viewer thinks that the algorithm manages to identify all the blocking artifact distortions on the image which have been captured by the viewer's eye. The subjective experiment was conducted for around 15 people and the Mean Perfomance Score (MPS) was calculated from each performance score of the
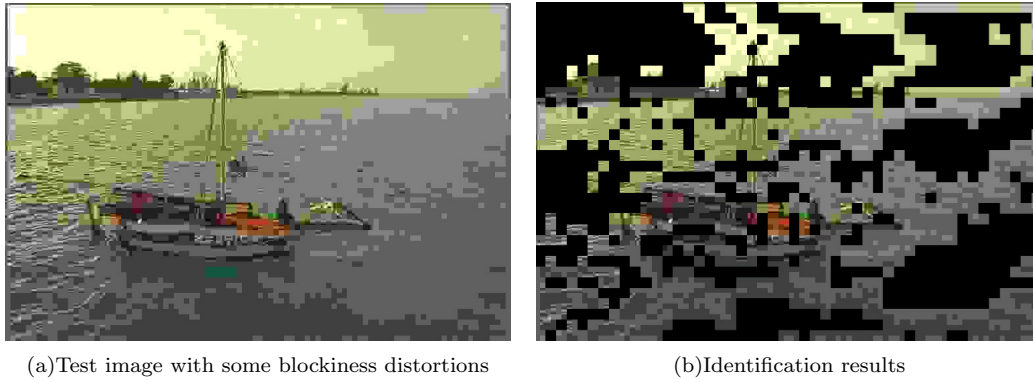
(a)Test image with some blockiness distortions   (b)Identification results

Fig.4: *Example of experimental results on blockiness distortion detection. Black areas on the identification results are those that do not contain blockiness artifacts.*
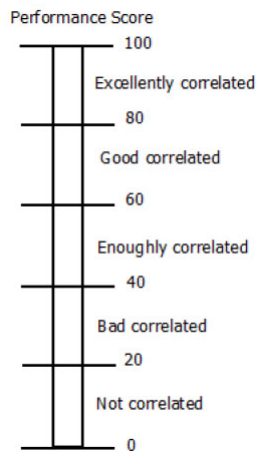

Fig.5: *Scoring method for subjective experiment*

Table 2: *Result summary of the subjective experiments for locating blockiness identification algorithm.*

Type	MPS	Std. Deviation
Overall	81.5	14.3
Good	81.3	14.1
Mid-To-Bad	81.4	13
Very Bad	85.4	11.8
Blurred	77.8	18.4

'Very Bad' image category which has smallest standard deviation of 11.8.

To demonstrate the accuracy and the effectiveness of the blockiness identification algorithm, we also present comparisons of the experimental results between JPEG and JPEG2000 images. The JPEG2000 coding will introduce distortion in form of blur or ringing artifacts but not in form of blockiness distortions. Therefore, the blockiness identification algorithm should be able to verify this, i.e. no blockiness should be detected on JPEG2000 encoded images. Some examples of our identification are described below.

In these examples, we used images from "Parrots" category of LIVE Image Database. Figure 6(a)-6(h) illustrate the experiments of our proposed method to locate blockiness distortions. Figure 6(a) shows a good-quality JPEG image, whilst 6(c) shows a bad-quality JPEG Image. Figure 6(b) and 6(d) illustrate the result of our proposed method for Parrots image in 6(a) and 6(c) respectively. The proposed method was also applied to JPEG2000 category images shown in Figure 6(e) and 6(g) for the original good and bad quality JPEG2000 image, respectively. In a JPEG2000 coded image, the distortions mainly come in form of blur or ringing, hence, no blockiness should be found on the image. Figure 6(f) and 6(h) demonstrate the results of our proposed method for the JPEG2000 images which confirm that our blockiness identification method did not make mistake by identifying blur or ringing artifacts. These results show that the proposed method has managed to
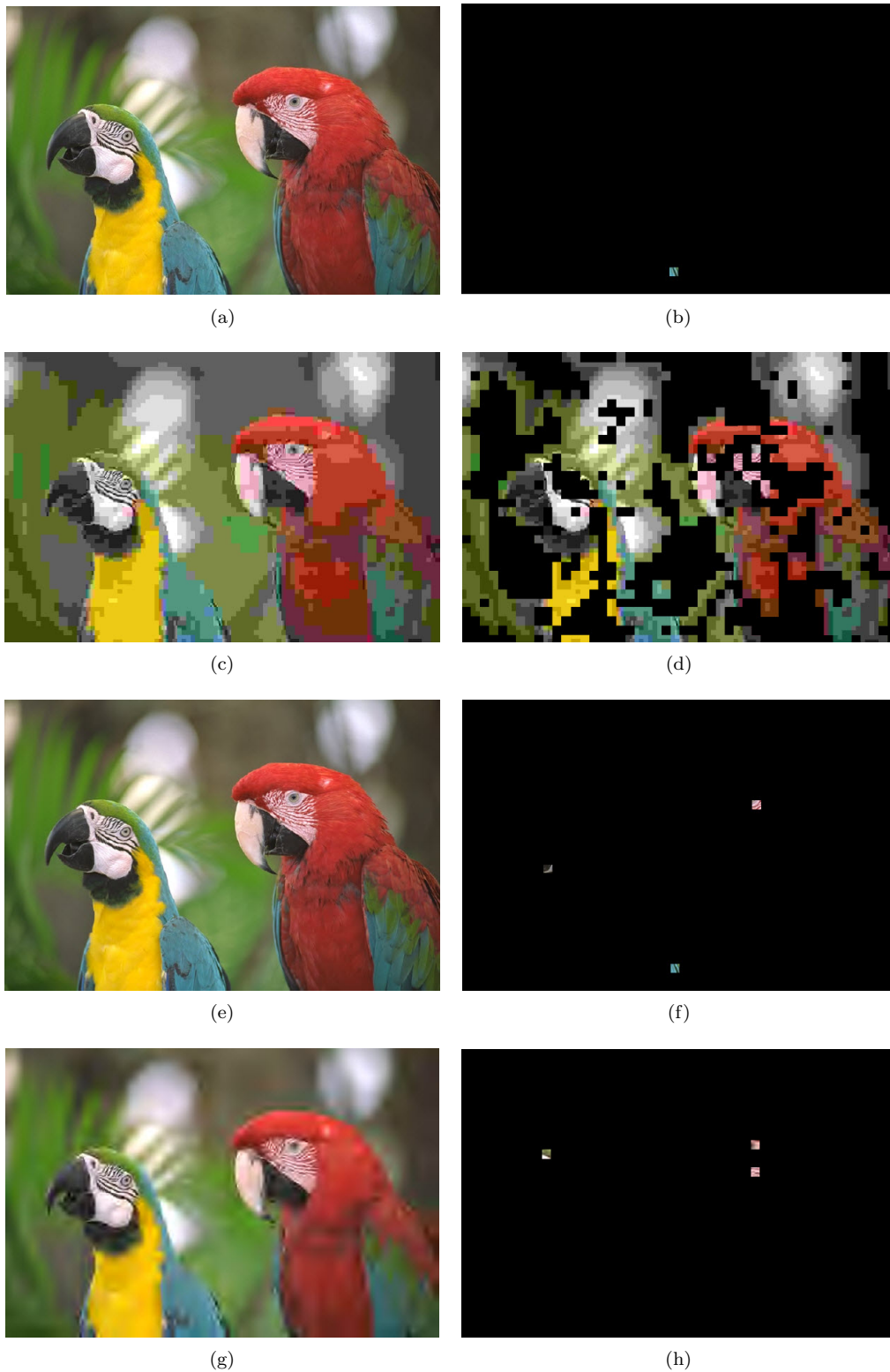
viewers. There were 30 images consisted of 12 good quality image, 6 mid-to-bad quality image, 6 very bad JPEG images, and 6 blurred JPEG2000 images used in the subjective experiment.

Table 2 summarizes the results of our subjective experiments. We can see that in general the algorithm shows 81.5 MPS that falls in 'Excellently correlated' category. We also present the categorized MPS for good, mid-to-bad, very bad, and blurred images respectively. The results show that most of the MPS for each category falls into 'Excellently correlated' except for the Blurred category which falls into 'Good correlated' category. The highest MPS is obtained for 'Very Bad' category of JPEG images, showing that the algorithm works really well when identifying severely compressed JPEG images. By analysing the Standard Deviation for each category, the standard deviation of the MPS for blurred category is the highest compared to the other. Thus, we can assume that some of the viewers have a really different perspective when they assess the algorithm performance for blurred images. This leads to a lower MPS for Blurred category images. As for the other categories, the Standard deviation is almost similar, excepts in

Fig.6: *Experiments of locating blockiness algorithm using "Parrots" Category image from LIVE JPEG Image Database. (a) Original good quality JPEG Image. (b) Result of blockiness identification from (a). The blockiness distortions is shown as a non-zero pixels. (c) Original bad quality JPEG Images. (d) Result of blockiness identification from (c). (e) Original good quality JPEG2000 Image. (f) Result of blockiness identification of (e). (g) Original bad quality JPEG2000 Image (h) Result of blockiness identification from (g).*
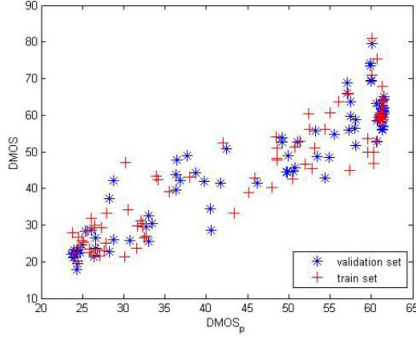
Fig.7: *Fitted Quality Metric plotted against LIVE JPEG DMOS*

identify blockiness distortions that appear on blocky JPEG images as expected, whilst ignoring any other types of distortions such as those that present on JPEG2000 encoded images.

Based on several experiments described above, we can conclude that the algorithm performs remarkably well and produces good identification results that correlate well with human's perceived view with an overall MPS of 81.5.

3.2 Objective Quality Metric

For the objective JPEG quality metric experiments, the four parameters that optimize the logistic curve function using non-linear regression must be calculated. To estimate the parameters of the logistic curve, we divided the image into training set and test (or validation) set. The test set was comprised of 15 categories of LIVE JPEG images, whereas the training set consisted of the remaining 14 categories. The *nlinfit* function from MATLAB was used to estimate the parameters. We set the initial parameter based on [20]. Using the non-linear regression method on the trainig set, the parameters were found as follows: $b_1 = 62.2023$, $b_2 = 22.9012$, $b_3 = 7.1471$, and $b_4 = 0.2521$. The validation set was then used to compute the final correlation between subjective data and the prediction using the parameters above.

Figure 7 shows the scatter plot of the fitted quality metric against the LIVE JPEG DMOS. It is easy to verify that the algorithm yields good results. Table 3 summarizes the comparison between our proposed method and some other published quality metrics in terms of the correlation values. Our method has achieved Pearson Correlation (PC) 0.93 and Spearman Correlation (SC) 0.89 overall. It is clear that the proposed method outperforms Harmonic gain method from LHS and PSNR. The latter is a full-reference framework whilst the former is a reduced-reference one. Our proposed method is also comparable to other NR methods such as LABM and NPBM [7], although ours is slightly below NPBM (particularly the Spearman correlation value).

Table 3: *Results of objective quality metric for JPEG image experiments*

Type	PC	SC
Proposed Method	0.93	0.89
Gain from LHS [6]	0.85	0.93
LABM [7]	0.83	0.84
NPBM [7]	0.94	0.92
PSNR	0.87	0.89

However, the superiority of our algorithm lies in the ability to detect and identify blockiness artifact locations and performing quality assessment in a single approach which is simpler than NPBM. For NPBM, the HVS implementation is computed twice each for horizontal and vertical direction involving two kinds of filter: texture and luminance filter. The transfer function that is used to implement HVS in NPBM is a pixel based operation.

For our algorithm, we only implement edge transformation using Sobel Operator and perform the HVS implementation directly to the edge image. Texture filtering is the process that costs the computational power most which is computed every 8×8 blocks. In contrast, in NPBM almost all of the metric is computed on a pixel based operation, which leads to more complex and time consuming process as image size gets bigger. On the other hand, our quality metric used block based operation to compute the metric which is derived from $\widehat{\phi}_i^{max}(p, q)$. Not only it has lower complexity than other methods, the block-based operation in our proposed method also lends itself to summarization of the feature such as used in reduced-reference framework. This opens up a possibility to use the proposed NR method in a hybrid RR/NR setting. The investigation into using these features in an RR framework, however, is out of the scope of this paper.

4. CONCLUSION AND FUTURE WORKS

In this paper, we present a novel method based on HWT analysis to identify blockiness distortions and assess the quality of JPEG images. The performance of our method shows promising results since it correlates well with subjective DMOS data of LIVE JPEG Database, with Pearson and Spearman correlations of 0.93 and 0.89, respectively. The algorithm to locate and identify blockiness distortions also performs remarkably well and agrees with the human perceived view indicated by a good performance score (81.5) obtained from subjective experiment.

Future works of this research may include performance improvement of the algorithm, for example, in texture filtering process. Further investigation on using the method in a hybrid RR/NR framework is also in progress. Application to video coding as well as adaptive block-size transform coding method will

also be considered.

5. ACKNOWLEDGEMENT

The authors wish to thank the anonymous reviewers for their recommendations to improve the quality of this paper.

References

[1] Zhou Wang and Alan Conrad Bovik, "A universal image quality index," *IEEE Signal Processing Letters*, vol. 9, no. 3, pp. 81–84, 2002.

[2] Zhou Wang, Alan Conrad Bovik, Hamid Rahim Seikh, and Eero P. Simoncelli, "Image quality assessment : From error visibility to structural similarity," *IEEE Transactions on Image Processing*, vol. 13, no. 4, pp. 600–612, 2004.

[3] Yung-Kai Lai and C.-C. Jay Kuo, "A haar wavelet approach to compressed image quality measurement," *International Journal of Visual Communication and Image Representation*, vol. 11, pp. 17–40, 2000.

[4] A. Bouzerdoum, A. Havstad, and E. Beghdadi, "Image quality assessment using a neural network approach," in *Proc. 4th IEEE International Symposium on Signal Processing and Information Technology*, 18–21 December 2004 2004, pp. 330 – 333.

[5] Kamrul Hasan Talukder and Koichi Harada, "Haar wavelet based approach for image compression and quality assessment of compressed image," *IAENG International Journal of Applied Mathematics*, vol. 36, no. 1, February 2007.

[6] Irwan Prasetya Gunawan and Mohammed Ghanbari, "Image quality assessment based on harmonics gain/loss information," in *IEEE International Conference on Image Processing*, 2005, pp. 429–432.

[7] Hantao Liu and Ingrid Heynderickx, "A perceptually relevant no-reference blockiness metric based on local image characteristics," *EURASIP Journal on Advances in Signal Processing*, 2009.

[8] Ming Goo Choi, Jung Hoon Jung, and Jae Wook Jeon, "No-reference image quality assessment using blur and noise," *International Journal of Computer Science and Engineering*, vol. 3:2, pp. 76–80, 2009.

[9] Yunkou Horita, Shinji Arata, and Tdakuni Murai, "No-Reference Image Quality Assessment for JPEG/JPEG2000 Coding," in *European Conference on Signal Processing*, 2004.

[10] Mohd. Haroon Khan, Athar A. Moinuddin, Ekram Khan, and Mohammed Ghanbari, "No-reference image quality assessment of wavelet coded images," in *Proceedings of 2010 IEEE 17th International Conference on Image Processing*, 2010.

[11] P. Marziliano, F. Dufaux, S. Winkler, and T. Ebrahimi, "No-reference perceptual blur metric," in *IEEE International Conference on Image Processing*, 2002.

[12] Irwan Prasetya Gunawan, *Reduced-Reference Impairment Metrics for Digitally Compressed Video*, Ph.D. thesis, University of Essex, 2006.

[13] G.A. Triantafyllidis, D. Tzovaras, and M.G. Strintzis, "Blockiness detection in compressed data," in *IEEE International Conference on Acoustics, Speech, and Signal Processing*, 2001, vol. 3, pp. 1533–1536.

[14] Hanghang Tong, Mingjing Li, Hongjiang Zhang, and Changsui Zhang, "Blur detection for digital images using wavelet transform," in *IEEE Conference of Multimedia and Expo*, 2004, pp. 17–20.

[15] Ingrid Daubechies, "Ten lectures on wavelets," *SIAM*, vol. 61, pp. 194–202, 1994.

[16] Hamid Rahim Seikh, Zhou Wang, Lo Cormack, and Alan Conrad Bovik, "Live image quality assessment database release 2," Available [Online], 2006.

[17] I. Sobel and G. Feldman, "A 3x3 isotropic gradient operator for image processing," in *Pattern Classification and Scene Analysis*. 1968, vol. 73, pp. 271–272, John Wiley and Sons.

[18] Stefan Winkler, "Issues in vision modelling for perceptual video quality assessment," *IEEE Signal Processing Letters*, vol. 78, no. 2, pp. 231–252, October 1999.

[19] Stephane G. Mallat, "A theory for multiresolution signal decomposition : The wavelet representation," *IEEE Transactions on Pattern Analysis and Machine Intelligence*, vol. 11, no.7, no. 674-693, 1989.

[20] "RRNR-TV Group Test Plan Draft Version 1.6," Tech. Rep., Video Quality Expert Group, May 2004.

Irwan Prasetya Gunawan received a bachelors degree with honours in electrical engineering from Sekolah Tinggi Teknologi Telkom (now Institut Teknologi Telkom), Bandung, Indonesia in 1996 with the final year of his undergraduate study (1995-1996) was spent in the Cable and Wireless College, Coventry, U.K. He received a masters degree in telecommunications engineering from the RMIT (Royal Melbourne Institute of Technology) University, Melbourne, Australia, in 1998, and the Ph.D in multimedia electronic systems engineering from the University of Essex, Colchester, United Kingdom, in 2006.

He was a Postdoctoral Researcher in the Department of Computing Science, University of Glasgow, U.K., in 2006-2008 to work on IP-RACINE project, a European Commission funded research project on digital cinema. He was a Lecturer in Sekolah Tinggi Ilmu Komputer Surabaya, Institut Teknologi Telkom Bandung, and Universitas Multimedia Nusantara Serpong Tangerang, before he joined Bakrie University as an academic in the Department of Information Technology early 2011. Before he started his academic career, he worked in the telecommunication industry with PT Telekomunikasi Indonesia Divisi Regional V Surabaya, East Java. He was a member

of the Institute of Electrical and Electronics Engineer (IEEE) Indonesian Chapter, including its Circuit and Systems Society and Communications Society. He was also active as the IEEE Indonesian Section Officer in the Professional Activities department in 2009. He is a member of Editorial Board for International Journal of Image Processing and Telkomnika (Indonesian Journal of Electrical Engineering). He has been a reviewer for several international journals such as IEEE Transactions on Circuit and Systems for Video Technology, IEEE Transactions on Broadcasting, Signal Processing: Image Communications, IET Electronics Letters, and Advanced in Multimedia, as well as reviewer for conferences such as ISWPC'07 (International Symposium on Wireless Pervasive Computing), ICTEL'08 (International Conference on Telecommunications), ICICI-BME (International Conference on Instrumentation, Communications, Information Technology and Biomedical Engineering) 2009, ICACSIS (International Conference on Advanced Computer Science and Information Systems) 2009-2010, etc. He has also served as member of the technical program committee and session chair for several of these international conferences. He was the Program Chair for the International Workshop on Advanced Image Technology (IWAIT) 2011 that was held in Jakarta, January 2011. He has coauthored several papers in international technical journals and conference proceedings, and written several popular newspaper articles in Bahasa Indonesia mostly centered around IT/telecommunication areas. His main research interests and expertise are quality assessment of digitally compressed image/video, various applications of digital image/video processing, super resolution, and multi-resolution analysis. His other interests include cryptography, computer security, and networking.

Dr. Gunawan is the co-recipient of best paper award at the 2002 APCC (Asia Pacific Conference on Communications) for his paper on image quality assessment. He was the recipient of a scholarship jointly funded by the British Council Indonesia, Cable and Wireless Indonesia, and the Cable and Wireless College, U.K., to spend his undergraduate's final year at the Cable and Wireless College, Coventry, U.K (1995-1996). He was awarded postgraduate research scholarship by the University of Essex via research grant from the British Telecoms Group CTO, U.K. during 2002-2005, for his Ph.D study. He held Cisco Certified Network Associate (CCNA) and Cisco Certified Design Associate (CCDA) certifications both acquired in 2001. He was trained in classical piano and once received a second prize award in a nation-wide classical piano competition. He also studied basic piano jazz briefly, and with his high school pop-jazz band took part and received a second prize in a nation-wide band competition.

Antony Halim received a B.S. degree in Computer Engineering from Universitas Multimedia Nusantara, Indonesian, in 2011. He is currently Web Programmer and Lecturer Assistant in Computer Engineering Department at Universitas Multimedia Nusantara. His research interests develop a web-based control panel for Rising Force game.